AAS 13-803

BROAD-SEARCH ALGORITHMS FOR THE SPACECRAFT TRAJECTORY DESIGN OF CALLISTO-GANYMEDE-IO TRIPLE FLYBY SEQUENCES FROM 2024-2040, PART I: HEURISTIC PRUNING OF THE SEARCH SPACE

Alfred E. Lynam*

Triple flybys of the Galilean moons of Jupiter can capture a spacecraft into orbit about Jupiter or quickly adjust the Jupiter-centered orbit of an already captured spacecraft. Because Callisto does not participate in the Laplace resonance among Ganymede, Europa, and Io, triple flyby sequences involving gravity-assists of Callisto, Ganymede, and Io occur only aperiodically for limited time windows. An exhaustive search of triple-flyby trajectories over a 16-year period from 2024-2040 using "blind" searching would require 8,415,358 Lambert function calls to find only 127,289 possible triple flyby trajectories. Because most of these Lambert function calls would not converge to feasible solutions, it is much more efficient to prune the solution space using a heuristic algorithm and then direct a much smaller number of Lambert function calls to find feasible triple flyby solutions. The novel "Phase Angle Pruning Heuristic" is derived and used to reduce the search space by 99%.

INTRODUCTION

Gravity-assist flybys of planets and moons expedite the design of interplanetary space missions because they can dramatically reduce the amount of ΔV (and propellant mass) required to accomplish a spacecraft's mission. The Galileo[1, 2] and Cassini-Huygens[3, 4] missions each performed several planetary flybys of Earth and Venus before they left the inner solar system to travel to Jupiter and Saturn (via a gravity assist of Jupiter), respectively. These gravity-assist flybys increased the heliocentric orbital energy of the Galileo and Cassini-Huygens spacecraft such that they could reach their outer solar system destinations with a feasible amount of propellant. After arriving at Jupiter, the Galileo mission was able to perform 32 gravity-assist flybys of Jupiter's Galilean moons before it impacted Jupiter[5]. Cassini has already performed more than 100 gravity-assist flybys of Saturn's moons, and will continue to tour the Saturn system until 2017[6, 7]. For both Galileo and Cassini, each of these flybys had a dual purpose of modifying the Planet-centered orbit of the spacecraft and performing scientific analysis of the planetary moons (although Cassini's flybys of Saturn's smaller moons had only a negligible effect on its trajectory).

Between their heliocentric planetary tours and planet-centered satellite tours, the Galileo and Cassini-Huygens spacecraft had to perform propulsive maneuvers to capture into planet-centered

*Assistant Professor, Mechanical and Aerospace Engineering Department, West Virginia University, ESB, Evansdale Dr. Room G-70, Morgantown, WV 26506-6106. Member AIAA. Member AAS.

orbits. While the Cassini-Huygens spacecraft simply performed a large maneuver at its closest approch to Saturn [4], the Galileo spacecraft performed a gravity-assist flyby of Io before it propulsively captured into orbit about Jupiter. This Io gravity assist reduced the propulsive ΔV required to capture Galileo into orbit about Jupiter by 175 m/s.[8] Combining gravity-assist(s) of a planetary satellite with a propulsive maneuver to capture a spacecraft into a planetary orbit is called "satellite-aided capture". Using a single satellite gravity-assist (as in the Galileo case) is called "single-satellite-aided capture", while using gravity assists of two or three satellites is called double- or triple- satellite-aided capture, respectively. In addition to the Galileo mission designers, several other investigators [9]–[15] have made substantial contributions to the solution of the single-satellite-aided capture problem. Nock and Uphoff,[12] Johannesen and D'Amario,[16] Landau et al.[17], and Strange et al.[18] have performed some initial mission design of double-satellite-aided capture sequences at Jupiter. (Jupiter is the only planet that has multiple moons, the four Galilean moons, that have enough gravity to permit meaningful gravity-assist flybys.) Lynam et al.[19] and Lynam and Longuski[20] investigated the mission design of both double- and triple-satellite-aided capture trajectories. They showed that using double- or triple-satellite-aided capture could reduce the ΔV required to capture into Jupiter orbit even further: by 230 m/s or 350 m/s, respectively, compared to single-satellite-aided capture.

Lynam and Longuski[21] performed a preliminary navigational analysis of double- and triple-satellite-aided capture, determining that double flybys could be successfully navigated using ground-based radiometric navigation, but triple flybys would require precise and rapid navigation techniques (perhaps even autonomous navigation) to safely execute. In addition to satellite-aided capture, triple flybys can be implemented within Jupiter satellite tours to increase the number of science flybys[22] or modify the orbital elements of a Jupiter-centered orbit. While most of the previous work on triple flybys focuses on point-design solutions, this paper and Part II[23] focus on performing a broad search for a particular type of triple flyby (Callisto-Ganymede-Io triple flyby sequences) over a 16-year range of dates between 2024 and 2040. This paper details a heuristic pruning algorithm that can eliminate impossible trajectories and reduce the search space by 99%, while the companion paper describes the broad-search Lambert algorithm that is used to find triple flyby trajectories within the reduced solution space. Part II also describes a promising triple-satellite-aided capture trajectory that would arrive at Jupiter in December 2029.

METHODOLOGY

Circular, Coplanar, Ephemeris-Free, Patched-Conic Model

The first step in developing the pruning heuristic is to analyze the Callisto-Ganymede-Io triple flyby problem using the simplest possible trajectory model. In this initial model, the orbits of the Galilean moons are modeled to be circular and coplanar with orbital radii equal to their semi-major axes. The spacecraft's orbit is modeled as four separate elliptical or hyperbolic two-dimensional conic sections in the same plane as the Galilean moons. The four conic sections are: the spacecraft's initial orbit from its apojove or its incoming asymptote (depending on whether the orbit is initially elliptical or hyperbolic) to the orbital radius of Callisto, the spacecraft's orbit from Callisto's to Ganymede's orbital radius, the spacecraft's orbit from Ganymede's to Io's orbital radius, and the spacecraft's orbit from Io's orbital radius to its next apojove or outgoing asymptote (depending on whether the final orbit is elliptical or hyperbolic). The four conic sections are patched together by modeling hyperbolic gravity-assist flybys of Callisto, Ganymede, and Io at their respective orbital radii. This patched-conic method is also termed "ephemeris free" because the orbital positions

of Callisto, Ganymede, and Io are modeled to always be coincident with the spacecraft's position as it flys across each moon's orbit; the positions of the moons with regard to absolute time (their ephemerides) are ignored. This approach is similar to that used by Lynam et al.[19] and Lynam and Longuski[22] to find Laplace-resonant triple flybys.

The inputs for the simplified patched-conic model are the initial semimajor axis (a) and eccentricity (e) of the incoming spacecraft. The spacecraft is propagated to its Callisto flyby via the conic equation, the vis-viva equation, and the definition of flight path angle:[24]

$$\cos\nu = \frac{a(1-e^2)-r}{e\,r} \tag{1}$$

$$V = \sqrt{\frac{2\mu_{\text{Jup}}}{r} - \frac{\mu}{a}} \tag{2}$$

$$\cos\gamma = \sqrt{\frac{a^2(1-e^2)}{r(2a-r)}} \tag{3}$$

where μ_{Jup} is the gravitational parameter of Jupiter, r is the radius of Callisto's orbit, ν is the spacecraft's true anomaly before the flyby, V is the spacecraft's speed before the flyby, and γ is the spacecraft's flight path angle before the flyby. The two-dimensional flyby solution is computed by finding the v-infinity, the pump angles, and the hyperbolic turning angle:[25]

$$V_\infty = \sqrt{V^2 + V_{Ca}^2 - 2V\,V_{Ca}\cos\gamma} \tag{4}$$

$$\cos\alpha_{\text{in}} = \frac{V^2 - V_{Ca}^2 - V_\infty^2}{2V_\infty V_{Ca}} \tag{5}$$

$$\sin(\delta/2) = \frac{\mu_{\text{Ca}}}{\mu_{\text{Ca}} + (R_{\text{Ca}} + h_{\text{p,Ca}})V_\infty} \tag{6}$$

$$\alpha_{\text{out}} = \alpha_{\text{in}} \pm \delta \tag{7}$$

where V_∞ is the hyperbolic excess velocity of the spacecraft with respect to Callisto, V_{Ca} is Callisto's orbital speed, α_{in} and α_{out} are the incoming and outgoing pump angles of the flyby, δ is the hyperbolic turning angle of the flyby, μ_{Ca} is the gravitational parameter of Callisto, R_{Ca} is the physical radius of Callisto, and $h_{\text{p,Ca}}$ is the flyby altitude of the spacecraft. The $\pm$ in Eq. 7 indicates that the flyby could either be an energy-reducing flyby or an energy-increasing flyby.

After the Callisto flyby is modeled, the orbital parameters of the spacecraft's transfer from Callisto to Ganymede can be calculated, the Ganymede flyby can be modeled, the orbital parameters of the transfer from Ganymede to Io can be calculated, and the Io flyby can be modeled. These calculations use similar equations to Eqs. 1–7, so they will not be discussed in detail. However, the semi-latus recta (p) and times of flight (T) of the Callisto-Ganymede and Ganymede-Io transfers must also be calculated because they are used as initial guesses in the Lambert algorithm used in Part II[23].

$$p = a(1 - e^2) \tag{8}$$

$$T = \sqrt{a^3/\mu_{\text{Jup}}}\,[E_2 - e\sin E_2 - (E_1 - e\sin E_1)] \tag{9}$$

$$T = \sqrt{-a^3/\mu_{\text{Jup}}}\,[e\sinh H_2 - H_2 - (e\sinh H_1 - H_1)] \tag{10}$$

where E_1, E_2, H_1 and H_2 are the elliptical and hyperbolic anomalies of the spacecraft at the beginning and end of its transfer between moons (depending on whether the transfer is elliptic or hyperbolic).

The final outputs of this circular, coplanar, patched-conic model are the phase angles (angular separations) between Ganymede and the other two moons at the time of the Ganymede flyby. These phase angles are of fundamental importance to the pruning heuristic developed in this paper because they are used to screen the relatively few feasible triple-flyby sequences from the entire solution space (of mostly infeasible sequences).

$$\Delta\lambda_{\text{Ca,Ga}} = (\nu_1 - \nu_2) + n_{\text{Ca}} T_{\text{Ca,Ga}} \tag{11}$$

$$\Delta\lambda_{\text{Ga,Io}} = (\nu_3 - \nu_4) + n_{\text{Io}} T_{\text{Ga,Io}} \tag{12}$$

where $\Delta\lambda_{\text{Ca,Ga}}$ is the angle from Ganymede's position to Callisto's position at the time of the Ganymede flyby, $\Delta\lambda_{\text{Ga,Io}}$ is the angle from Io's position at the time of the Ganymede flyby to Ganymede's position, $T_{\text{Ca,Ga}}$ is the spacecraft's transfer time between Callisto and Ganymede, and $T_{\text{Ga,Io}}$ is the spacecraft's transfer time between Ganymede and Io. Additionally, ν_1 is the true anomaly of the spacecraft immediately after the Callisto flyby, ν_2 is the true anomaly of the spacecraft before the Ganymede flyby, ν_3 is the true anomaly of the spacecraft after the Ganymede flyby, ν_4 is the true anomaly of the spacecraft before the Io flyby. (ν_2 and ν_3 are slightly different because the Ganymede flyby alters the true anomaly of Jupiter-centered orbit of the spacecraft.) Figure 1 depicts the phase angles $\Delta\lambda_{\text{Ca,Ga}}$ and $\Delta\lambda_{\text{Ga,Io}}$ in the context of a triple flyby.

Interpolation Models for Data Pruning

The circular, coplanar, ephemeris-free, patched-conic model was implemented in MATLAB, and its inputs and outputs are summarized in Table 1. The range of input values for the initial orbital elements (a and e) was chosen such that it included both Jupiter-centered, elliptical orbits and Jupiter-centered, incoming hyperbolic asymptotes with V_∞ of less than 6 km/s. The flyby altitudes are modeled as always being 100 km for Callisto, 1,500 km for Ganymede, and 300 km for Io. The Callisto flyby is lower than the others because it is least likely to have navigational errors.[21] The Ganymede flyby is much higher than the others because of limitations in the circular, coplanar model. In the full three-dimensional model, much of equivalent ΔV of the Ganymede flyby is often needed to change the inclination of the spacecraft's orbit so it can reach Io for a flyby. This inclination-change requirement results in a loss of equivalent ΔV for orbital energy change, which is modeled in two-dimensions by an artificial increase in the flyby altitude at Ganymede.

In addition to the orbital parameter inputs in Table 1, a number of qualitative inputs are used to distiguish between four distinct sets of Callisto-Ganymede-Io triple flyby solutions. The flyby

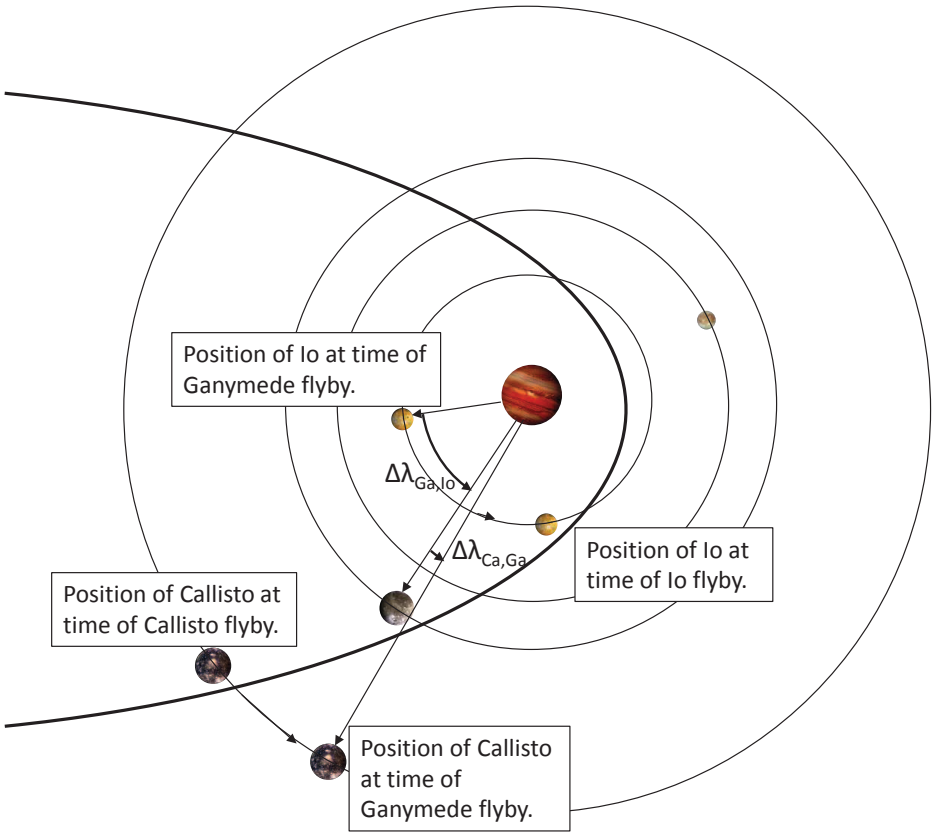

Figure 1. A geometric definition of the Callisto-Ganymede and Ganymede-Io phase angles for a Callisto-Ganymede-Io triple flyby.

Table 1. Circular, Coplanar, Ephemeris-free, Patched-conic Model: Inputs and Outputs

Inputs	Range of Input Values	Outputs
Initial Semimajor Axis (a), km[a]	-1.7×10^6 to 1.2×10^6	$p_{\text{Ca,Ga}}$
Initial Eccentricity (e)	0.6 to 1.3	$p_{\text{Ga,Io}}$
Callisto Flyby Type	Energy-reducing	$T_{\text{Ca,Ga}}$
Callisto Flyby h_{p}, km	100	$T_{\text{Ga,Io}}$
Ganymede Flyby Type	Energy-increasing OR Energy-reducing	$\Delta\lambda_{\text{Ca,Ga}}$
Ganymede Flyby h_{p}, km	1500	$\Delta\lambda_{\text{Ga,Io}}$
Io Flyby Type	Energy-reducing	—
Io Flyby h_{p}, km	300	—
Io Flyby Position[b]	Before Perijove OR After Perijove	—

[a] Since parabolas have an infinite semimajor axis, the semimajor axis range goes from -1.7×10^6 down to $-\infty$ and from $+\infty$ down to 1.2×10^6 rather than directly from -1.7×10^6 to 1.2×10^6 through 0.

[b] The Callisto and Ganymede flybys always occur before the spacecraft's perijove in this model.

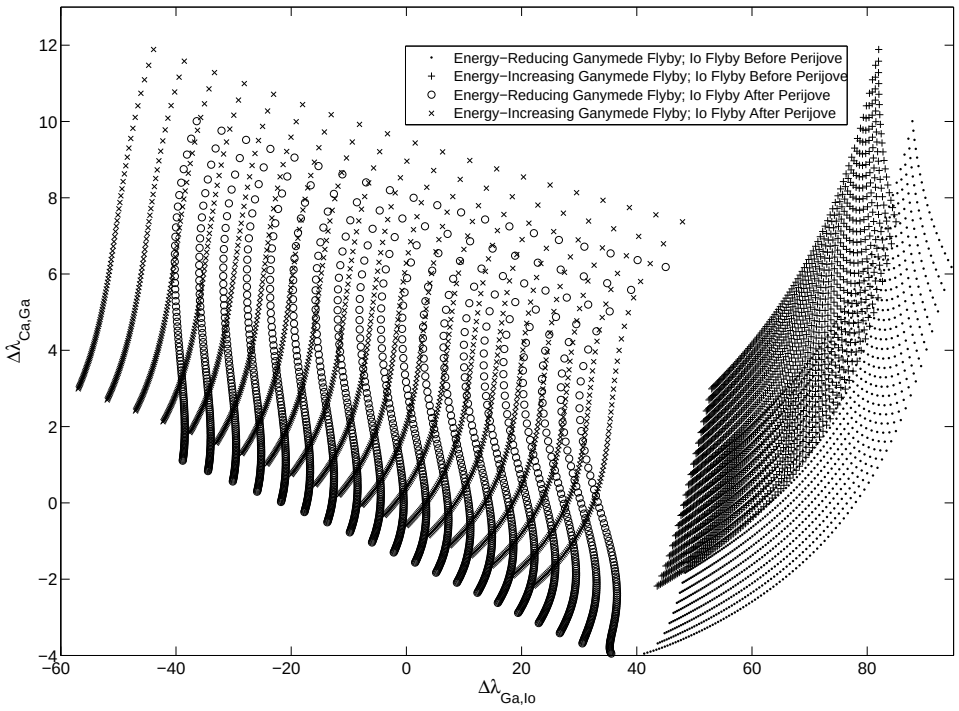

Figure 2. The Callisto-Ganymede and Ganymede-Io phase angles (in degrees) for each set of patched-conic propagations.

of Ganymede could potentially be either energy-increasing or energy-reducing, and the flyby of Io could occur either before the spacecraft's perijove or after the spacecraft's perijove. (While the flybys of Callisto and Io could technically be either energy-increasing or energy-reducing, this paper focuses on the cases where they are always energy-reducing.)

For each of the four cases, the initial orbital elements are varied within a MATLAB array to create 1,780 two-dimensional, patched-conic trajectories. In the context of the reduction heuristic, the outputs are the semi-latus recta and times of flight of the Callisto-Ganymede and Ganymede-Io transfers (see Eqs. 8–10), and the Callisto-Ganymede and Ganymede-Io phase angles (see Eqs. 11 and 12). The phase angle outputs from the four sets of 1,780 patched-conic propagations are plotted in Fig. 2.

In Fig. 2, each of the four sets of 1780 patched-conic propagations roughly forms a quadrilateral in phase-angle space. Since the four sides are not linear, polynomial interpolation is used to form four curves that approximately bound each set of propagations. Figure 3 shows these polynomial curves bounding each set of phase angle data. Boolean expressions are generated using these polynomial curves in order to form the pruning heuristic. The Boolean expressions have the following general form:

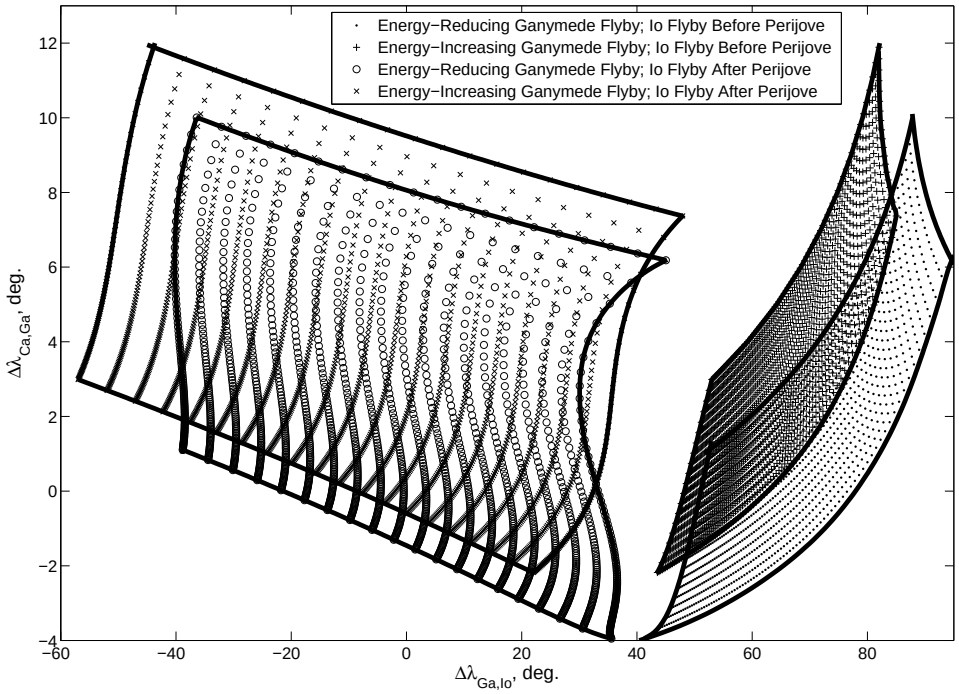

Figure 3. Bounding polynomial curves (thick black lines) for each set of phase angle data.

$$
\begin{aligned}
PruningBoolean = &\left(\Delta\lambda_{\text{Ga,Io}} \leq b_0 + b_1\Delta\lambda_{\text{Ca,Ga}} + ... + b_n\Delta\lambda^n_{\text{Ca,Ga}}\right) \\
&\;\&\; \left(\Delta\lambda_{\text{Ga,Io}} \geq c_0 + c_1\Delta\lambda_{\text{Ca,Ga}} + ... + c_n\Delta\lambda^n_{\text{Ca,Ga}}\right) \\
&\;\&\; \left(\Delta\lambda_{\text{Ca,Ga}} \leq f_0 + f_1\Delta\lambda_{\text{Ga,Io}} + ... + f_n\Delta\lambda^n_{\text{Ga,Io}}\right) \\
&\;\&\; \left(\Delta\lambda_{\text{Ca,Ga}} \geq g_0 + g_1\Delta\lambda_{\text{Ga,Io}} + ... + g_n\Delta\lambda^n_{\text{Ga,Io}}\right)
\end{aligned}
\tag{13}
$$

where b_i, c_i, f_i, and g_i are coefficients for the Boolean polynomials, and $\&$ represents the boolean AND operator. There are four different pruning booleans which each represent one of the four sets of trajectories. If one of the four pruning booleans is TRUE for a given set of phase angles ($\Delta\lambda_{\text{Ca,Ga}}$ and $\Delta\lambda_{\text{Ga,Io}}$), then the trajectory represented by those phase angles is feasible. If all of the four pruning booleans are FALSE, then the trajectory represented by those phase angles is known to be infeasible and discarded without further analysis. Since certain areas of the four pruning booleans are overlapping (see Fig. 3), some sets of phase angles may have two solutions depending on whether the spacecraft's Ganymede flyby is energy-reducing or energy-increasing. This multiplicity of solutions is handled implicitly during the Lambert solution process in Part II[23].

In addition to the polynomial interpolation structures that bound the phase-angle results of the propagations, interpolation structures are also created for the semi-latus rectum and time of flight outputs for the Callisto-Ganymede and Ganymede-Io transfers. Nearest-neighbor, two-dimensional interpolation structures are created from the trajectory propagations for each of the four outputs ($p_{\text{Ca,Ga}}$, $p_{\text{Ga,Io}}$, $T_{\text{Ca,Ga}}$, and $T_{\text{Ga,Io}}$) with the two phase angles ($\Delta\lambda_{\text{Ca,Ga}}$ and $\Delta\lambda_{\text{Ga,Io}}$) as the dependent

variables. Since the data is scattered, MATLAB's "TriScatteredInterp" function is used to create the two-dimensional interpolation structures. These structures are later used in Part II[23] to extract initial guesses for $p_{\text{Ca,Ga}}$, $p_{\text{Ga,Io}}$, $T_{\text{Ca,Ga}}$, and $T_{\text{Ga,Io}}$.

Ephemeris Reading, Phase Angle Calculation, and Data Reduction

After the Boolean Expressions for the phase angles ($\Delta\lambda_{\text{Ca,Ga}}$ and $\Delta\lambda_{\text{Ga,Io}}$) and the interpolation structures for $p_{\text{Ca,Ga}}$, $p_{\text{Ga,Io}}$, $T_{\text{Ca,Ga}}$, and $T_{\text{Ga,Io}}$ are generated, ephemeris reading is used to find the positions of the Galilean moons over time. The positions of Callisto, Ganymede, and Io are extracted from the ephemeris file jup230l.bsp[26] in 1-minute increments over 8 2-year invervals between 2024 and 2040. (The 16-year interval must be divided into 8 2-year invervals because of contiguous array length limits in MATLAB; there are about 1.05 million minutes in a 2-year period.) After the position vectors of the moons are extracted, the approximate orbit normal vector for the three moons is calculated using consecutive positions of Ganymede. Although the three moons are not in the exact same orbit plane, they are all within one degree of inclication of each other. Also, this orbit normal is only used to provide a positive angular direction for the phase angle calculations, so it is only important that this orbit normal be approximately correct.

$$\hat{\mathbf{n}} = \frac{\vec{\mathbf{r}}_{\text{Ga,1}} \times \vec{\mathbf{r}}_{\text{Ga,2}}}{\|\vec{\mathbf{r}}_{\text{Ga,1}} \times \vec{\mathbf{r}}_{\text{Ga,2}}\|} \tag{14}$$

where $\hat{\mathbf{n}}$ is the orbit normal for Ganymede's orbit, $\vec{\mathbf{r}}_{\text{Ga,1}}$ is the first extracted ephemeris position of Ganymede, and $\vec{\mathbf{r}}_{\text{Ga,2}}$ is an extracted ephemeris position of Ganymede 19 minutes after the first position. After the orbit normal is calculated, the two phase angles are calculated at a particular time with the following expressions involving the scalar triple product, the signum function, and the geometric definition of a dot product:

$$\Delta\lambda_{\text{ephem,Ca,Ga}} = Sgn\left(\hat{\mathbf{n}} \bullet \vec{\mathbf{r}}_{\text{Ga}} \times \vec{\mathbf{r}}_{\text{Ca}}\right) \cos^{-1}\left(\frac{\vec{\mathbf{r}}_{\text{Ga}} \bullet \vec{\mathbf{r}}_{\text{Ca}}}{\|\vec{\mathbf{r}}_{\text{Ga}}\| \, \|\vec{\mathbf{r}}_{\text{Ca}}\|}\right) \tag{15}$$

$$\Delta\lambda_{\text{ephem,Ga,Io}} = Sgn\left(\hat{\mathbf{n}} \bullet \vec{\mathbf{r}}_{\text{Io}} \times \vec{\mathbf{r}}_{\text{Ga}}\right) \cos^{-1}\left(\frac{\vec{\mathbf{r}}_{\text{Io}} \bullet \vec{\mathbf{r}}_{\text{Ga}}}{\|\vec{\mathbf{r}}_{\text{Io}}\| \, \|\vec{\mathbf{r}}_{\text{Ga}}\|}\right) \tag{16}$$

where $\Delta\lambda_{\text{ephem,Ca,Ga}}$ and $\Delta\lambda_{\text{ephem,Ga,Io}}$ are the Callisto-Ganymede and Ganymede-Io phase angles calculated from the ephemerides at a particular time, $\vec{\mathbf{r}}_{\text{Ca}}$, $\vec{\mathbf{r}}_{\text{Ga}}$, and $\vec{\mathbf{r}}_{\text{Io}}$ are the position vectors of the three moons at a particular time, the signum function and the triple scalar product ensure that the signs of the phase angles are consistent with Eqs. 11 and 12, and the arccosines of the unit dot products of the position vectors are used to calculate the magnitude of the phase angles.

Once the phase angles are calculated using Eqs. 15 and 16 for each of the 1.05 million minutes for a 2-year period, all four sets of boolean expressions described by Eq. 13 are applied to each pair of phase angles. If one or two of the four boolean expressions is true for a particular pair of phase angles, the time associated with that pair of phase angles is recorded as a feasible Ganymede flyby time, and one or two sets of $p_{\text{Ca,Ga}}$, $p_{\text{Ga,Io}}$, $T_{\text{Ca,Ga}}$, and $T_{\text{Ga,Io}}$ initial guesses are extracted from the interpolation structures for use in the Lambert solution in Part II[23]. If there are two boolean expressions that are true for the same pair of phase angles, then the two solutions are implicitly distiguished in the Lambert solver because they have different initial guesses for $p_{\text{Ca,Ga}}$, $p_{\text{Ga,Io}}$, $T_{\text{Ca,Ga}}$, and $T_{\text{Ga,Io}}$.

Table 2. Data Reduction of Time Vectors

Ganymede Flyby	Io Flyby	Vector Length	% of Minutes
Combined Minutes in 16-years	—	8.42×10^6	100%
Energy-Reducing	Before PJ	14,747	0.175%
Energy-Increasing	Before PJ	11,052	0.131%
Energy-Reducing	After PJ	45,512	0.541%
Energy-Increasing	After PJ	55,978	0.665%
Total Reduced Times	—	127,289	1.513%
Unique Reduced Times	—	82,110	0.976%
Impossible Times Pruned	—	8.33×10^6	99.024%

RESULTS

As mentioned in the methodology section, the 16-year date range is split up into 2-year intervals in order to reduce the MATLAB vector sizes to feasible levels. Each 2-year interval contains about 1.05 million minutes, position vectors from three moons are extracted, and each position vector contains 3 elements, so the total number of double-precision, floating-point numbers extracted from the ephemeris file is about 9.45 million per 2-year interval. Once these position vectors are extracted, Eqs. 14–16 are used to calculate $\Delta\lambda_{\text{ephem,Ca,Ga}}$ and $\Delta\lambda_{\text{ephem,Ga,Io}}$ for each minute, resulting in 2.10 million phase angles per 2-year period. The $\Delta\lambda_{\text{ephem,Ca,Ga}}$ and $\Delta\lambda_{\text{ephem,Ga,Io}}$ phase angle data are used to form four pruning booleans calculated from Eq. 13 for each of the four regions in Fig. 3. These four reduction booleans are used to compress each 1.05 million entry time vector into four much smaller time vectors by removing all of the times that would never correspond to a triple flyby. The process is performed independently for all eight 2-year periods between 2024 and 2040. After each 2-year period, the four reduced time vectors generated for that period are aggregated to those of the previous periods. After all eight of the 2-year periods are processed, the four aggregated time vectors represent the available times for each of the four triple flyby categories represented by Fig. 3.

The combined number of minutes that are analyzed in the 16-year period are 8.41 million. The lengths of the four aggregated time vectors are compared to the total combined number of minutes in Table 2. As indicated by Fig. 3, the solution space for Io flybys before perijove in Table 2 is much smaller than the solution space for Io flybys after perijove. As also indicated by Fig. 3, there are large areas of overlap between the energy-reducing Ganymede flybys and the energy-increasing Ganymede flybys: 55,179 of the 82,110 unique times have two triple flyby solutions with differing Ganymede flybys. These instances of double solutions are dealt with implicitly by using separate interpolation structures for the semilatus rectum, p, and time of flight, T, initial guesses for the energy-reducing and energy-increasing solutions. The key result of Table 2 (and of this paper) is that the data pruning heuristic was able to reduce the solution space by 99%, thereby eliminating a substantial number of impossible solutions before the Lambert solution process is attempted.

The algorithm described in the methodology section was implemented in MATLAB on a desktop PC with 2 Intel Xeon CPU E5-2687W @ 3.10 GHz processors. Vectorization was used heavily to optimize the MATLAB code. Although parallelization, using compiled code instead of MATLAB,

Table 3. Computational time of MATLAB Data Reduction code segments

Code Segment	Comp. time (s)	% of Comp. Time
Total Runtime	167.459	100%
CCEFPC model	0.132	0.079%
Interpolation structures	0.239	0.143%
Ephemeris reading	162.773	97.202%
Phase angle calculation and data reduction	4.315	2.577%

or using faster ephemeris readers than SPICE could have been used to speed up the calculations, the single-core vectorized MATLAB implementation was sufficient to solve the data reduction problem in a reasonable amount of time. The primary computational bottleneck was using SPICE to read the position vectors of Callisto, Ganymede, and Io from jup230l.bsp for 8.42 million minutes. Running the circular, coplanar, ephemeris-free, patched conic (CCEFPC) model; creating the interpolation structures; calculating the phase angles from the position vectors; and reducing the data using the pruning heuristic required very little computational time as indicated by Table 3.

DISCUSSION

The primary advantage of the pruning heuristic as a global trajectory optimization method is that it can detect a limited number of feasible solutions within an enormously large solution space. The phase angle pruning heuristic is particularly effective for triple flybys in the Jupiter system for several reasons. First, the orbits of the Galilean moons have low eccentricity and inclination, so the circular, coplanar assumption is relatively accurate for the Jupiter system. Second, the three flybys occur in rapid succession, so there is less time for error to accumulate in the patched-conic model. Third, triple flybys are heavily geometrically constrained, and the pruning heuristic allows those constraints to be expressed directly in equations.

In addition to the Callisto-Ganymede-Io triple flybys, there are also three other classes of triple flybys involving Callisto, Ganymede, and Io: Callisto-Io-Ganymede triple flybys, Ganymede-Io-Callisto triple flybys, and Io-Ganymede-Callisto triple flybys. Although this paper focuses on Callisto-Ganymede-Io triple flybys, the reduction heuristic could be applied to any feasible combination of three of Jupiter's Galilean moons. Lynam et al.[19, 20] describes a similar phase angle analysis for triple flybys of the three participants in the Laplace resonance: Ganymede, Europa, and Io. However, other combinations of the Galilean moons such as Callisto-Ganymede-Europa and Callisto-Europa-Io triple flybys have not yet been explored.

Another potential astrodynamics application of the pruning heuristic would be to find triple flybys of Uranus's moons. Uranus's four most massive moons (Titania, Oberon, Umbriel, and Ariel) are much less massive than the Galilean moons, so the gravity-assist capacity of a triple flyby would be lessened. However, Uranus's moons are also in roughly circular, co-planar orbits around Uranus, so the methodology and mathematics of the pruning heuristic for triple flybys should apply to them also. It is also possible that the pruning heuristic could be applied to triple flybys of Venus, Earth, and Mars. Although it would be noticeably less accurate because of the inclinations of the orbits

of Venus and Mars, the pruning heuristic could potentially be used to find Earth-Venus-Earth-Mars gravity assist trajectories to the outer solar system.

CONCLUSIONS

Callisto-Ganymede-Io triple flybys can be used to capture a spacecraft into orbit about Jupiter or quickly adjust the Jupiter-centered orbital elements of an already captured spacecraft. The phase angle reduction heuristic developed in this paper was capable of reducing the solution space of Callisto-Ganymede-Io triple flybys from 2024–2040 by removing 99% of the infeasible solutions. The remaining 1% of the solutions are potentially feasible and can be calculated using a Lambert solver. The interpolation structures for semi-latus rectum and transfer times for the Callisto-Ganymede and Ganymede-Io transfers can be used to as initial guesses for the solution of Lambert's problem. Overall, the methods used in this paper dramatically expedite the search for triple flybys of Callisto, Ganymede, and Io by eliminating infeasible solutions and providing initial guesses for Lambert solutions.

REFERENCES

[1] C. Potts and M. Wilson, "Maneuver Design for the Galileo VEEGA Trajectory," *AAS Paper 93-566, Proceedings of the AAS/AIAA Astrodynamics Specialist Conference*, Victoria, B.C., Canada, Aug. 1993.

[2] T. Barber, F. Krug, and B. Froidevaux, "Initial Galileo Propulsion System In-Flight Characterization," *AIAA Paper No: 93-2117, Proceedings of the AIAA/SAE/ASME/ASEE 29th Joint Propulsion Conference and Exhibit*, Monterrey, CA, June 1993.

[3] T. D. Goodson, D. L. Gray, Y. Hahn, and F. Peralta, "Cassini Maneuver Experience: Finishing Inner Cruise," *AAS Paper 00-167, Proceedings of the AAS/AIAA Spaceflight Mechanics Meeting*, Clearwater, FL, January 2000.

[4] D. Roth, P. Antreasian, J. Bordi, K. Criddle, R. Ionasescu, R. Jacobson, J. Jones, M. C. Meed, I. Roundhill, and J. Stauch, "Cassini Orbit Reconstruction from Jupiter to Saturn," *AAS Paper 05-311, Proceedings of the AAS/AIAA Astrodynamics Specialist Conference*, Lake Tahoe, CA, August 2005.

[5] R. Haw, P. Antreasian, T. McElrath, and G. Lewis, "Galileo Prime Mission Navigation," *Journal of Spacecraft and Rockets*, Vol. 39, 2000, pp. 56–63.

[6] C. G. Ballard, J. Arrieta, Y. Hahn, P. W. Stumpf, S. V. Wagner, and P. N. Williams, "Cassini Maneuver Experience: Ending the Equinox Mission," *AIAA Paper 2010-8257, AIAA/AAS Astrodynamics Specialists Conference*, Toronto, ON, CA, August 2010.

[7] P. N. Williams, C. G. Ballard, E. M. Gist, T. D. Goodson, Y. Hahn, P. W. Stumpf, and S. V. Wagner, "Flight Path Control Design for the Cassini Equinox Mission," *Proceedings of the AAS Spaceflight Mechanics Meeting*, Savannah, GA, February 2009.

[8] M. G. Wilson, C. L. Potts, R. A. Mase, C. A. Halsell, and D. V. Byrnes, "Manuever Design for Galileo Jupiter Approach and Orbital Operations," *Space Flight Dynamics, Proceedings of the 12th International Symposium*, Darmstadt, Germany, June 1997, pp. 1–9.

[9] R. W. Longman, "Gravity Assist from Jupiter's Moons for Jupiter-Orbiting Space Missions," tech. rep., The RAND Corp., Santa Monica, CA, 1968.

[10] R. W. Longman and A. M. Schneider, "Use of Jupiter's Moons for Gravity Assist," *Journal of Spacecraft and Rockets*, Vol. 7, No. 5, May 1970, pp. 570–576.

[11] J. K. Cline, "Satellite Aided Capture," *Celestial Mechanics*, Vol. 19, May 1979, pp. 405–415.

[12] K. T. Nock and C. Uphoff, "Satellite Aided Orbit Capture," *AAS Paper 79-165, Proceedings of the AAS/AIAA Astrodynamics Specialist Conference*, Provincetown, MA, June 25–27, 1979.

[13] M. Malcolm and C. McInnes, "Spacecraft Planetary Capture Using Gravity-Assist Maneuvers," *Journal of Guidance, Control, and Dynamics*, Vol. 28, March-April 2005, pp. 365–368.

[14] C. H. Yam, *Design of Missions to the Outer Planets and Optimization of Low-Thrust, Gravity-Assist Trajectories via Reduced Parameterization*. PhD thesis, School of Aeronautics and Astronautics, Purdue University, West Lafayette, IN, May 2008, pp. 96–104.

[15] M. Okutsu, C. H. Yam, and J. M. Longuski, "Cassini End-of-Life Escape Trajectories to the Outer Planets," *AAS Paper 07-258, Proceedings of the AAS/AIAA Astrodynamics Specialist Conference*, Mackinac Island, MI, August 2007.

[16] J. R. Johannesen and L. A. D'Amario, "Europa Orbiter Mission Trajectory Design," *AAS Paper 99-330, Proceedings of the AAS/AIAA Astrodynamics Conference*, Vol. 103, Girdwood, AK, August 1999.

[17] D. Landau, N. Strange, and T. Lam, "Solar Electric Propulsion with Satellite Flyby for Jovian Capture," *Proceedings of the AAS/AIAA Spaceflight Mechanics Conference*, San Diego, CA, February 2010.

[18] N. Strange, D. Landau, R. Hofer, J. Snyder, T. Randolph, S. Campagnola, J. Szabo, and B. Pote, "Solar Electric Propulsion Gravity-Assist Tours For Jupiter Missions," *AIAA Paper No: 2012-4518, Proceedings of the AIAA/AAS Astrodynamics Specialists Conference*, Minneapolis, MN, August 2012.

[19] A. E. Lynam, K. W. Kloster, and J. M. Longuski, "Multiple-satellite-aided Capture Trajectories at Jupiter using the Laplace Resonance," *Celestial Mechanics and Dynamical Astronomy*, Vol. 109, No. 1, 2011.

[20] A. E. Lynam and J. M. Longuski, "Interplanetary Trajectories for Multiple Satellite-Aided Capture at Jupiter," *Journal of Guidance, Control, and Dynamics*, Vol. 34, No. 5, September-October 2011.

[21] A. E. Lynam and J. M. Longuski, "Preliminary Analysis for the Navigation of Multiple-satellite-aided Capture Sequences at Jupiter," *Acta Astronautica*, 2012.

[22] A. E. Lynam and J. M. Longuski, "Laplace-Resonant Triple-Cyclers for Missions to Jupiter," *Acta Astronautica*, Vol. 69, No. 3-4, August 2011.

[23] A. Lynam, "Broad-search Algorithms for the Spacecraft Trajectory Design of Callisto-Ganymede-Io Triple Flyby Sequences from 2024-2040, Part II: Lambert Pathfinding and Trajectory Solutions," *Proceedings of the AAS/AIAA Astrodynamics Specialists Conference*, Hilton Head, SC, August 2013.

[24] D. Vallado, *Fundamentals of Astrodynamics and Applications, 3rd edition*. New York, NY: Springer, 2007.

[25] N. Strange, R. Russell, and B. Buffington, "Mapping the V-infinity Globe," *AAS Paper No: 07-277, Proceedings of the AAS/AIAA Astrodynamics Specialists Conference*, Mackinac Island, MI, August 2007.

[26] R. A. Jacobson, "Jup230 - JPL satellite ephemeris," ssd.jpl.nasa.gov/?sat_ephem, 2003.